Hydrogen adsorption on Zn–BDC, Cr–BDC, Ni–DABCO, and Mg–DOBDC metal–organic frameworks

ARTICLE *in* JOURNAL OF CHEMICAL & ENGINEERING DATA · NOVEMBER 2013

Impact Factor: 2.04 · DOI: 10.1021/je400546d

5 AUTHORS, INCLUDING:

Prashant Mishra
Indian Institute of Technology Guwahati
8 PUBLICATIONS **38** CITATIONS
SEE PROFILE

Satyannarayana Edubilli
Indian Institute of Technology Guwahati
5 PUBLICATIONS **38** CITATIONS
SEE PROFILE

Anil Verma
Indian Institute of Technology Delhi
35 PUBLICATIONS **261** CITATIONS
SEE PROFILE

Sasidhar Gumma
Indian Institute of Technology Guwahati
32 PUBLICATIONS **415** CITATIONS
SEE PROFILE

Journal of chemical & engineering data

Article

pubs.acs.org/jced

Hydrogen Adsorption on Zn-BDC, Cr-BDC, Ni-DABCO, and Mg-DOBDC Metal−Organic Frameworks

Debjyoti Sahu,[†] Prashant Mishra,[‡] Satyannarayana Edubilli,[‡] Anil Verma,[†,‡] and Sasidhar Gumma*[,†,‡]

[†]Centre for Energy, Indian Institute of Technology Guwahati and [‡]Department of Chemical Engineering, Indian Institute of Technology Guwahati, Guwahati, 781039, Assam, India

Supporting Information

ABSTRACT: This work reports hydrogen adsorption properties of four different metal−organic frameworks (MOFs) namely Zn-BDC, Cr-BDC, Ni-DABCO, and Mg-DOBDC. Gravimetric hydrogen adsorption measurements are performed over a wide range of temperature (90 K to 298 K) and pressure (0 bar to 100 bar). At the lowest experimental temperature (90 K to 100 K) all the isotherms are saturated and the adsorption capacity is governed by pore volume. On the other hand, at room temperature the isotherms closely follow Henry's law. Modeling of the excess isotherms is also done. Net adsorption isotherms, which can directly indicate the efficiency of porous adsorbent for storage, are also presented. In terms of volumetric efficiency, Mg-DOBDC MOF exhibits best storage capacity out of all the MOFs considered in this study.

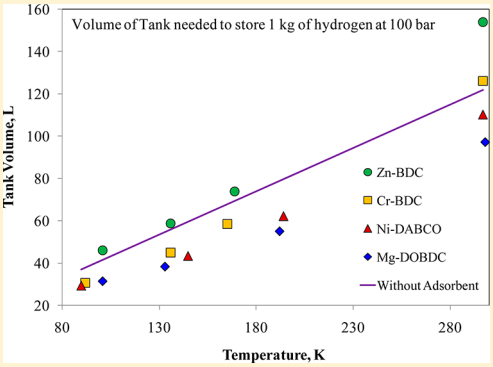

1. INTRODUCTION

Many countries have recognized the hydrogen-based energy system as a partial substitute to the conventional oil-based system. Depleting resources of fossil fuel may reduce production and supply in the future. Air pollution is a collateral damage while using fossil fuel. Hydrogen-based fuel may overcome some of these environmental impacts as it is a lightweight flammable gas. However, hydrogen storage poses a serious challenge. The US DOE[1,2] hydrogen storage target for 2015 is about 9 wt % of the adsorbent (and 81 g L^{-1} volumetric storage capacity) considering a refueling range in excess of 300 miles. Moreover, future generation cars may be lightweight and more fuel efficient; therefore, lower values than the target may be realistic. While, hydrogen storage capacity of traditional porous materials like carbons[3,4] and zeolites,[5,6] etc. has been studied for a long time, interest in storage in metal−organic frameworks (MOFs) is a more recent phenomenon.

MOFs are porous material readily synthesized by coordinative bonding of metal atoms with organic linkers. These materials are widely being investigated for their potential application in gas separation, gas storage, and catalysis.[7−14] Adsorption characteristics in MOFs depend on the geometry of the linker as well as the saturation (coordinated) level of the metal atom. MOFs have gained attention over other conventional materials because of their high surface area, larger pore volume, and tunable structure. However, some MOFs degrade on exposure to water vapor.[15] Adsorption isotherms of hydrogen on various porous materials such as activated carbons, zeolites, or MOFs are reported mainly at ambient temperature and at 77 K. A comparison of sample literature for hydrogen storage on some MOFs, zeolites, and allotropes of carbon is elaborated in Table 1.

In general, high pressure hydrogen adsorption data for cryogenic temperatures above 77 K is relatively limited.[16,23,24] An alternative to very low temperature storage/adsorption of hydrogen (and physically realizable target in near future) is to store it at an intermediate temperature. Moreover, study of hydrogen adsorption properties at the intermediate temperatures help in understanding the effect of various characteristics of porous solids and in the design and development of "tuned" materials to enhance hydrogen storage capacity.

The measurement of hydrogen storage on porous solids is a nontrivial task. The calculation of the pore and impenetrable solid volume may introduce considerable error[31] in estimating the amount of adsorbed hydrogen. These quantities (viz. solid volume and pore volume) are used during buoyancy corrections for obtaining excess and absolute adsorption, respectively. In net adsorption measurements, the use of these volumes is avoided[31] and reduces unnecessary confusion in estimation of the solid and pore volumes. Moreover, net adsorption accounts for the loss of volume (of the bulk gas phase) occupied by the impenetrable solid. Thus, net adsorption isotherm directly gives the additional amount of hydrogen that can be stored in a tank containing adsorbent compared to that of an empty tank at the same temperature and pressure.

In this work, excess hydrogen adsorption isotherms are reported at several intermediate temperatures between 90 K and 298 K over a wide pressure range. In addition, for the reasons discussed earlier, hydrogen adsorption is also reported

Received: June 7, 2013
Accepted: October 1, 2013
Published: October 25, 2013

Table 1. Comparison of Hydrogen Uptake in Different Adsorbents for Different Temperatures

adsorbent	T/K	P/bar	wt %	ref	T/K	P/bar	wt %	ref
Cu-BTC	77	50	3.8	16	298	50	0.3	16
	175	50	1	16				
Cr-BTC	77	26.5	3.28	17	298	73	0.15	17
Co-DABCO	77	1	2.45	18	298	17.2	0.89	18
MIL 53	77	16	3.8	19	293	50	0.37	20
MOF 177	77	70	7.5	21	298	100	0.62	22
Ni-DOBDC	150	27	1.5	23				
Graphene	77	10	1.2	24	298	10	0.1	24
	123	10	0.6	24	173	10	0.25	24
CNT	77	1	0.8	25	298	60	0.14	25
Zeolite	77	15	2.19	5	303	30	0.3	25
Zn-BDC	77	20	4.5	10, 26	298	20	1, 0.05	10, 27
	101	20	0.85	this work	293	20	0.12	28
	136	20	0.6	this work	169	20	0.25	this work
Cr-BDC	77	80	6.1	17	297	80	0.43	17
	92	80	3.6	this work	297	80	0.42	this work
	136	80	2.5	this work	165	80	1.7	this work
Ni-DABCO	77	50	3.76	29	299	50	0.65	29
	90	50	3.39	this work	297	50	0.4	this work
	145	50	2.39	this work	194	50	1.2	this work
Mg-DOBDC	77	80	3.2	30	298	80	0.5	30
	101	80	3.6	this work	298	80	0.6	this work
	133	80	3.2	this work	192	80	2.4	this work

in terms of net adsorption, and its suitability for evaluating the performance of solid adsorbents is illustrated. The MOFs chosen for the study are Zn-BDC, Cr-BDC, Ni-DABCO, and Mg-DOBDC, which cover a wide range of physical characteristics (Table S1 in the Supporting Information).

2. EXPERIMENTAL SECTION

2.1. Material Synthesis and Characterization. The detailed procedures that were followed to synthesize the studied materials are provided in the Supporting Information. The synthesized materials are thoroughly characterized by performing TGA, XRD, and BET surface area analysis. These results closely match with that reported in earlier literature and are included in the Supporting Information.

2.2. Hydrogen Adsorption Measurement. Adsorption equilibria were measured gravimetrically using a magnetic suspension balance (Rubotherm). The adsorbents were activated prior to each isotherm measurement by heating it at 473 K under vacuum (and a purge flow of 20 cm^3 min^{-1} of helium). Equilibrium measurement was carried out as per the usual procedure.[32] For excess adsorption, adsorbent as well as bucket volume was used as buoyancy volume during buoyancy corrections. The buoyancy volume of the porous solid adsorbent sample was obtained using buoyancy measurement on the sample using helium as a nonadsorbing gas. However, for net adsorption only the bucket volume was used for buoyancy corrections. The density of hydrogen was taken from the NIST Web site[33] for the corresponding experimental conditions. Cryogenic temperatures were obtained using a mixture of methanol and liquid nitrogen.[34] During experiments, temperature fluctuations were within a range of ± 2 K. The intermittent addition of excess liquid nitrogen was done manually to maintain the desired temperature.

3. RESULT AND DISCUSSION

3.1. Excess Adsorption. Excess adsorption isotherms of hydrogen on Zn-BDC, Cr-BDC, Ni-DABCO, and Mg-DOBDC at four different temperatures are shown in Figures 1 to 4.

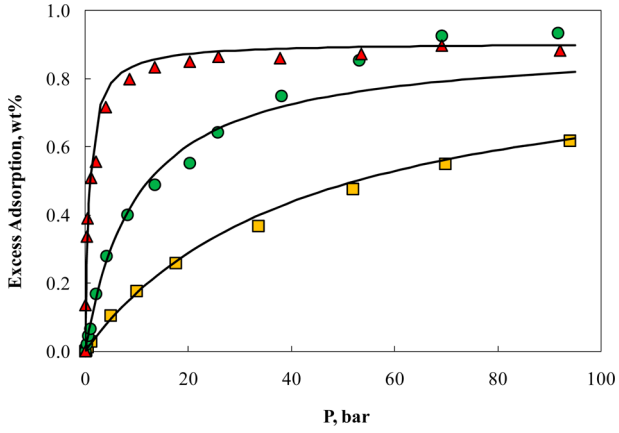

Figure 1. H_2 pressure composition isotherms of Zn-BDC. Symbols are excess adsorption from experimental data at red triangle, 101 K; green circle, 136 K; yellow square, 169 K. Lines are model fit to excess adsorption.

Isotherms of all the MOFs show saturation at 90 K to 100 K within our experimental pressure range. At room temperature, the isotherms were within the Henry region throughout the entire measurement. However, for intermediate temperature range (133 K to 194 K) even though saturation was not achieved, significant adsorption capacities were observed.

Saturation loading of hydrogen on Zn-BDC is 0.85 wt % at 20 bar and 101 K (Figure 1). This value is five times less compared to the loading reported by Yaghi's group[10] which is mainly due to the difference in the surface area and pore volume (see Table S1 in Supporting Information). Such

dx.doi.org/10.1021/je400546d | J. Chem. Eng. Data 2013, 58, 3096−3101

variations are not uncommon in the literature for Zn-BDC.[26,27] For Cr-BDC the saturation is 3.8 wt % at 45 bar and 92 K (Figure 2). Similarly, for Ni-DABCO the adsorption isotherm

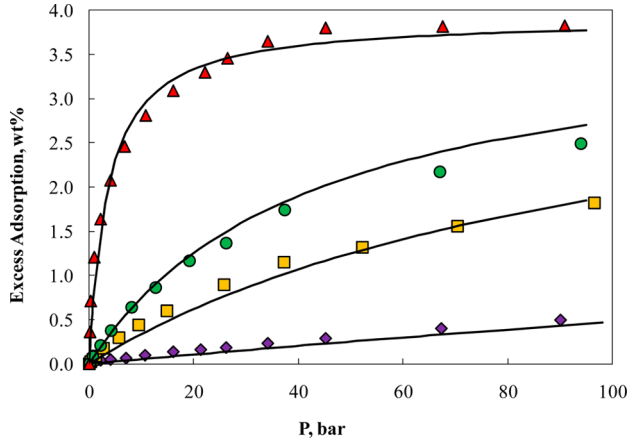

Figure 2. H_2 pressure composition isotherms of Cr-BDC. Symbols are excess adsorption from experimental data at red triangle, 92 K; green circle, 136 K; yellow square, 165 K; purple diamond, 297 K. Lines are model fit to excess adsorption.

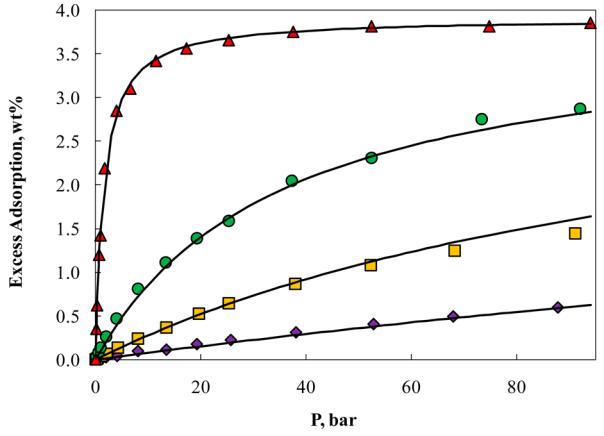

Figure 3. H_2 pressure composition isotherms of Ni-DABCO. Symbols are excess adsorption from experimental data at red triangle, 90 K; green circle, 145 K; yellow square, 194 K; purple diamond, 297 K. Lines are model fit to excess adsorption.

saturates at 3.65 wt % at 25 bar and 90 K (Figure 3). For Mg-DOBDC the adsorption isotherm saturates with 3.2 wt % loading at 25 bar and 101 K (Figure 4). At low temperature (92 K) maximum excess loading of 3.8 wt % was obtained for Cr-BDC due to its high pore volume compared to other considered MOFs. The saturation adsorption capacity for hydrogen on porous materials mostly depends on the pore volume[35] and results obtained in this study also indicate this relationship.

To better understand the effect of temperature on hydrogen adsorption, measurements were performed at intermediate temperatures. For Zn-BDC, the hydrogen loading increases from 0.47 wt % to 0.84 wt % at 50 bar when temperature changes from 169 K to 136 K (Figure 1). Similarly for Cr-BDC loading changes from 1.2 wt % to 1.8 wt % at ~40 bar when temperature changes from 165 K to 136 K (Figure 2). Similar

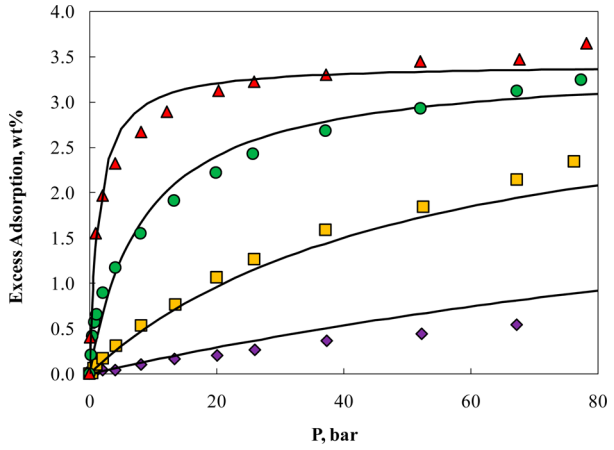

Figure 4. H_2 pressure composition isotherms of Mg-DOBDC. Symbols are excess adsorption from experimental data at red triangle, 101 K; green circle, 133 K; yellow square, 192 K; purple diamond, 298 K. Lines are model fit to excess adsorption.

changes in loading (1.6 wt % to 2.7 wt %) at ~40 bar are observed for Mg-DOBDC when temperature is reduced from 192 K to 133 K (Figure 4). However, Ni-DABCO exhibits a greater increment (0.9 wt % to 2.1 wt %) at ~40 bar when temperature decreases from 194 K to 145 K (Figure 3).

A simple Langmuir equation was sufficient to fit the experimental excess adsorption isotherms of all the MOFs. Langmuir equation can be represented as (eq 1):

$$W = \frac{W_{max} bP}{1 + bP} \quad (1)$$

where W is the amount adsorbed in wt %, P is the pressure in bar, and W_{max} is the saturation loading in wt %. Parameter b is the affinity constant and can be expressed in terms of temperature independent parameters b_0 and b_1 (eq 2). The fit parameters are given in Table 2.

$$b = b_0 \exp(b_1/T) \quad (2)$$

Table 2. Parameters for Fitted Langmuir Isotherm Model and Enthalpy of Adsorption at Zero Coverage

	maximum loading	affinity constant		adsorption enthalpy
adsorbent	W_{max}/wt %	$b_0 \cdot 10^4$/bar^{-1}	b_1/K	kJ mol^{-1}
Zn-BDC	0.905	0.584	1014	7.79
Cr-BDC	3.908	1.245	714	6.89
Ni-DABCO	3.907	1.665	744	5.6
Mg-DOBDC	3.416	3.369	780	7.96

The variation in Henry's constant with temperature is shown in Figure 5. As temperature increases from 90 K to 297 K, the difference between Henry's constants of all the four MOFs gradually decreases. Henry's constants of Mg-DOBDC and Cr-BDC at cryogenic temperature are slightly higher than that of other two MOFs; this could be possibly due to the presence of unsaturated metal sites in Mg-DOBDC and Cr-BDC. The enthalpies of adsorption at zero coverage (Table 2) were obtained from the change in Henry's constants with temperature.

3.2. Net Adsorption. Most of the hydrogen adsorption data in literature is reported either in terms of excess or

dx.doi.org/10.1021/je400546d | J. Chem. Eng. Data 2013, 58, 3096−3101

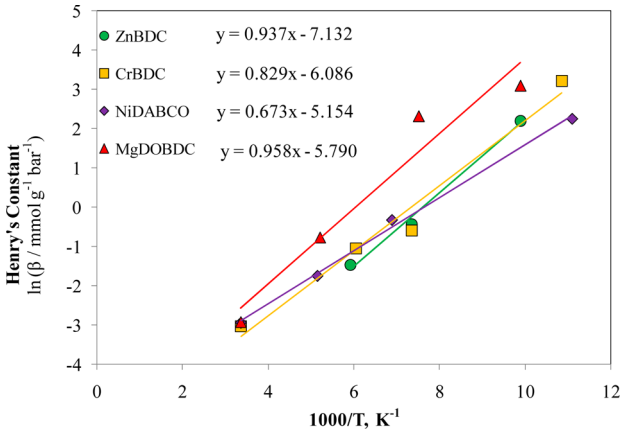

Figure 5. Henry's constant of all four metal−organic frameworks obtained from different isotherms: green circle, Zn-BDC; yellow square, Cr-BDC; purple diamond, Ni-DABCO; and red triangle, Mg-DOBDC. Lines are guide to eye.

absolute amount.[36] However, in both these representations, the volume loss corresponding to the volume of solid part of adsorbent is not considered. Any conclusion about advantage of using adsorbent for storage based on excess or absolute adsorption data may lead to wrong interpretations. Moreover, incorrect estimates of impenetrable solid volume lead to erroneous excess adsorption data; the error will be significant for low adsorbing species like hydrogen.

To avoid this confusion, all experimental measurements are directly converted into net adsorption values (Figures 6 to 9).[31]

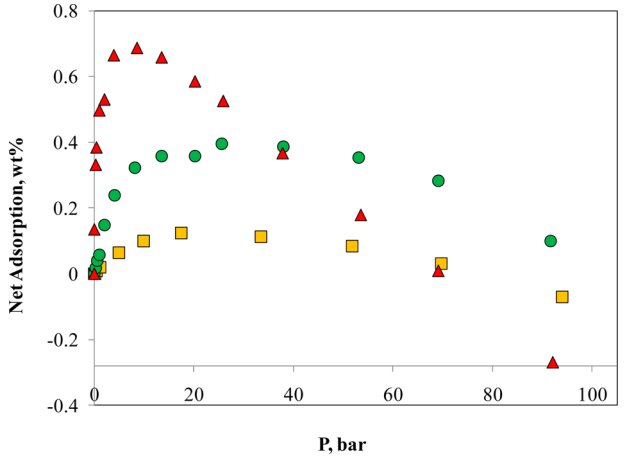

Figure 6. Net adsorption isotherms of Zn-BDC: red triangle, 101 K; green circle, 136 K; and yellow square, 169 K.

At room temperature, net adsorption for Cr-BDC and Ni-DABCO are close to zero, indicating that a tank containing Cr-BDC or a Ni-DABCO sample will store almost the same amount of hydrogen either in the presence or in the absence of the adsorbent material; that is, no additional benefit exists in using adsorbent for storage. However it must be noted that their excess loadings of 0.5 wt % and 0.6 wt % at 297 K and 90 bar (Figures 2 and 3) are quite decent. On the other hand, Mg-DOBDC, which contains open metal sites exhibits a significant positive net adsorption 0.32 wt % at 298 K and 80 bar (Figure 9) compared to the other MOFs; the presence of metal sites for room temperature hydrogen storage is now apparent. All MOFs in this study with the exception of Zn-BDC, exhibit a

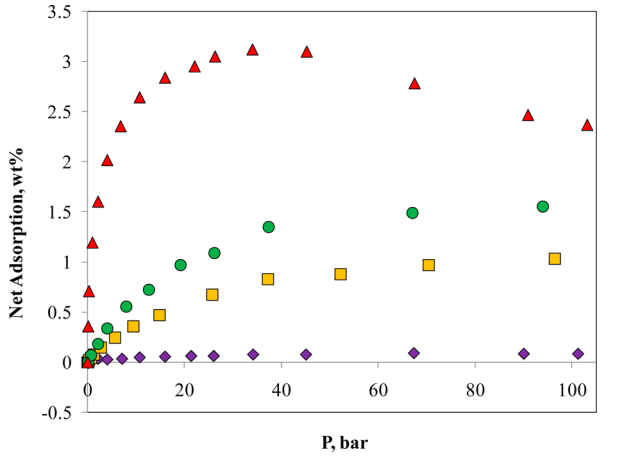

Figure 7. Net adsorption isotherms of Cr-BDC: red triangle, 92 K; green circle, 136 K; yellow square, 165 K; and purple diamond, 297 K.

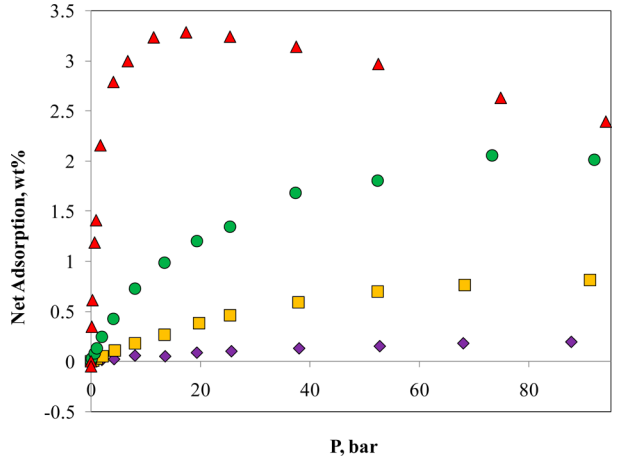

Figure 8. Net adsorption isotherms of Ni-DABCO: red triangle, 90 K; green circle, 145; yellow square, 194 K; and purple diamond, 297 K.

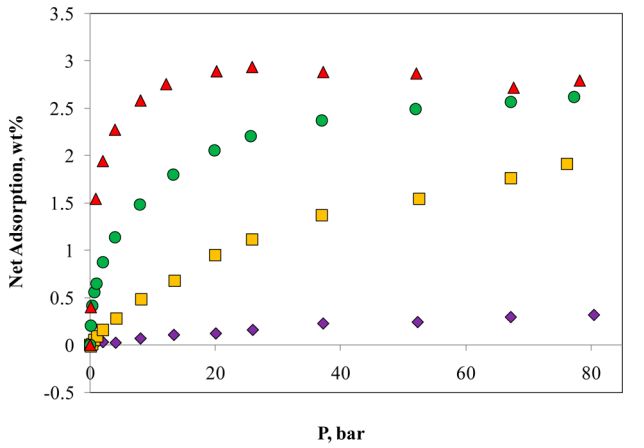

Figure 9. Net adsorption isotherms of Mg-DOBDC: red triangle, 101 K; green circle, 133 K; yellow square, 192 K; and purple diamond, 298 K.

maximum net adsorption uptake of about 3 wt % at the lowest experimental temperature.

Comparison of isotherms at intermediate temperatures suggests that presence of open metal sites plays a crucial role at low pressures. The highest net loading for the intermediate

dx.doi.org/10.1021/je400546d | J. Chem. Eng. Data 2013, 58, 3096−3101

temperature range was obtained for Mg-DOBDC as 1.9 wt % at 192 K and 75 bar (Figure 9). This value is almost twice than that for other MOFs thereby highlighting the usefulness of metal sites unsaturation for practical hydrogen storage applications.

3.3. Gas Storage. Hydrogen is a lightweight gas hence the volumetric storage capacity is rather important. Tank volume required to store say, 1 kg of hydrogen can give a clearer picture (minimum requirement to run in excess of 100 km[37]). Tank volumes needed to store 1 kg of H_2 at room temperature and at 100 bar pressure using four different MOFs are calculated using the net adsorption capacities directly and are shown in Figure 10. A tank filled with Zn-BDC will actually reduce the volumetric capacity of the tank. Even at a cryogenic temperature of 101 K the volume of the tank required increases from 41 (empty tank) to 46 L (filled with Zn-BDC). On the other hand, if the tank is filled with other MOFs (Cr-BDC, Ni-DABCO, or Mg-DOBDC), its volume decreases; the smallest volume required would be for the tank using Mg-DOBDC as adsorbent.

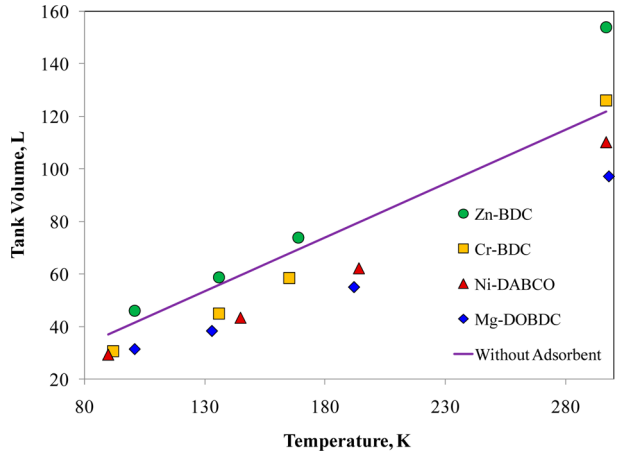

Figure 10. Tank volumes required to store 1 kg of H_2 with the following as adsorbent: green circle, Zn-BDC; yellow square, Cr-BDC; red triangle, Ni-DABCO; and blue diamond, Mg-DOBDC. Line represents empty tank.

Figure 11 shows the effect of Mg-DOBDC adsorbent on the volume of tank necessary to store 1 kg of hydrogen at different temperatures and 100 bar pressure. A similar comparison for other MOFs is given in the Supporting Information (Figures S4–S6). An empty tank of 122 L is required to store 1 kg of H_2 at 298 K and 100 bar, whereas the tank volume reduces to 97 L when filled with Mg-DOBDC. Similarly for 101 K and 100 bar, the tank volume decreases from 41 to 31 L. It was observed that over the temperature range of our measurements, the volume of the tank for hydrogen storage is reduced by about 20 % to 30 % by using Mg-DOBDC as an adsorbent.

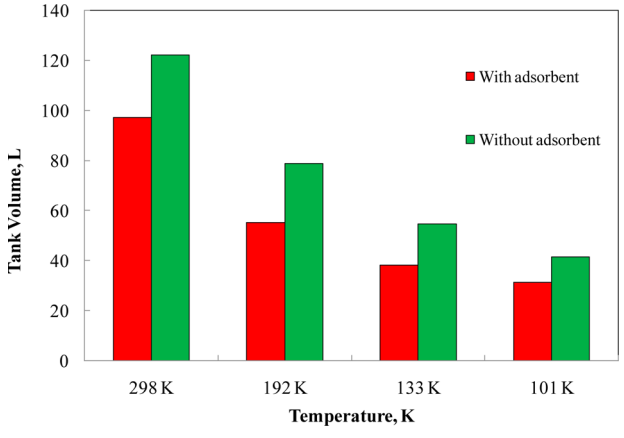

Figure 11. Tank volumes required to store 1 kg of hydrogen with Mg-DOBDC as adsorbent.

4. CONCLUSIONS

Four different types of MOFs namely Zn-BDC, Cr-BDC, Ni-DABCO, and Mg-DOBDC have been synthesized in our laboratory for hydrogen adsorption studies. Gravimetric adsorption measurement has been carried out between 90 K and 298 K. The effect of coordinatively unsaturated metal sites on the hydrogen adsorption characteristics was demonstrated with respect to temperature; it was observed that for experimental conditions where isotherms are not saturated, these unsaturated metal sites plays a major role during adsorption. On the other hand, saturation loadings are governed by pore volume. Net adsorption framework is suggested to avoid unnecessary confusion in determination of impenetrable solid volume and pore volumes and highlight the actual advantage of storing hydrogen in a tank containing adsorbent as compared to that in an empty tank.

■ ASSOCIATED CONTENT

Supporting Information

Detailed procedures that were followed to synthesize the studied materials; analysis results; additional tables and graphics as described in the text. This material is available free of charge via the Internet at http://pubs.acs.org.

■ AUTHOR INFORMATION

Corresponding Author

*Tel./Fax: +91 361 2582261. E-mail: s.gumma@iitg.ernet.in.

Notes

The authors declare no competing financial interest.

■ ACKNOWLEDGMENTS

The authors are thankful to Centre for Scientific and Industrial Research, New Delhi, India, for financial support through project Grant 01(2522)/11/EMR-II.

■ REFERENCES

(1) *DOE Hydrogen Program 2007 Annual Report*; DOE: Washington, DC, 2007; www.hydrogen.energy.gov/annual_progress07.html).

(2) *NREL/MP-150-42220*; DOE: Washington, DC, 2007; www.nrel.gov/docs/gen/fy08/42220.pdf.

(3) Panella, B.; Hirscher, M.; Roth, S. Hydrogen adsorption in different carbon nanostructures. *Carbon* **2005**, *43*, 2209.

(4) Campesi, R.; Cuevas, A.; Gadiou, B.; Leroy, E.; Hirscher, M.; Vix-Guterl, C.; Latroche, M. Hydrogen storage properties of Pd nanoparticle/carbon template composites. *Carbon* **2008**, *46*, 206.

(5) Langmi, H. W.; Book, D.; Walton, A.; Johnson, S. R.; Al-Mamouri, M. M.; Speight, J. D.; Edwards, P. P.; Harris, I. R.; Anderson, P. A. Hydrogen storage in ion exchanged zeolites. *J. Alloys Comp.* **2005**, *404–406*, 637.

(6) Czaja, A. U.; Trukhan, N.; Muller, U. Industrial applications of metal organic frameworks. *Chem. Soc. Rev.* **2009**, *38*, 1284.

(7) Li, H.; Eddaoudi, M.; Keeffe, M. O.; Yaghi, O. M. Design and synthesis of an exceptionally stable and highly porous metal-organic framework. *Nature* **1999**, *402*, 276.

(8) Yaghi, O. M.; Keeffe, M. O.; Ockwig, N. W.; Chae, H. K.; Eddaoudi, M.; Kim, J. Reticular synthesis and the design of new materials. *Nature* **2003**, *423*, 705.
(9) Yaghi, O. M.; Li, H.; Davis, C.; Richardson, D.; Groy, T. L. Synthetic strategies, structure patterns and emerging properties in the chemistry of modular porous solids. *Acc. Chem. Res.* **1998**, *31*, 474.
(10) Rosi, N. L.; Eckert, J.; Eddaoudi, M.; Vodak, D. T.; Kim, J.; Keefe, M. O.; Yaghi, O. M. Hydrogen storage in microporous metal-organic frameworks. *Science* **2003**, *300*, 1127.
(11) Chen, B.; Eddaoudi, M.; Hyde, S. T.; Keefe, M. O.; Yaghi, O. M. Interwoven metal-organic framework on a periodic minimal surface with extra-large pores. *Science* **2001**, *29*, 11021.
(12) Eddaoudi, M.; Moler, D. B.; Li, H.; Chen, B.; Reineke, T. M.; Keeffe, M. O.; Yaghi, O. M. Modular chemistry: Secondary building units as a basis for the design of highly porous and robust metal organic carboxylate frameworks. *Acc. Chem. Res.* **2001**, *34*, 319.
(13) Eddaoudi, M.; Li, H.; Yaghi, O. M. Highly porous and stable metal organic frameworks: Structure design and sorption properties. *J. Am. Chem. Soc.* **2000**, *122*, 1391.
(14) Fletcher, A. J.; Thomas, K. M.; Rosseinsky, M. J. Flexibility in metal organic framework materials: Impact on sorption properties. *J. Solid State Chem.* **2005**, *178*, 2491.
(15) Chowdhury, P.; Bikkina, C.; Gumma, S. Adsorption properties of the chromium based metal organic framework MIL-101. *J. Phys. Chem. C* **2009**, *113*, 6616.
(16) Liu, J.; Culp, J. T.; Natesakhawat, S.; Bockrath, B. C.; Zande, B.; Sankar, S. G.; Garberoglio, G.; Johnson, J. K. Experimental and theoretical studies of gas adsorption in $Cu_3(BTC)_2$: An effective activation procedure. *J. Phys. Chem. C* **2007**, *111*, 9305.
(17) Latroche, M.; Surble, S.; Serre, C.; Mellot-Draznieks, C.; Llewellyn, P. L.; Lee, J. H.; Chang, J. S.; Jhung, S. H.; Ferey, G. Hydrogen storage in the giant-pore metal–organic frameworks MIL-100 and MIL-101. *Angew. Chem., Int. Ed.* **2006**, *45*, 8227.
(18) Chun, H.; Jung, H.; Koo, G.; Jeong, H.; Kim, D. K. Efficient hydrogen sorption in 8-connected MOFs based on trinuclear pinwheel motifs. *Inorg. Chem.* **2008**, *47*, 5355.
(19) Férey, G.; Latroche, M.; Serre, C.; Millange, F.; Loiseau, T.; Guégan, A. P. Hydrogen adsorption in the nanoporous metal-benzenedicarboxylate $M(OH)(O_2C–C_6H_4–CO_2)$($M = Al^{3+}$, Cr^{3+}), MIL-53. *Chem. Commun.* **2003**, *24*, 2976.
(20) Liu, Y. Y.; Zeng, J. L.; Zhang, J.; Xu, F.; Sun, L. X. Improved hydrogen storage in the modified metal-organic frameworks by hydrogen spillover effect. *Int. J. Hydrogen Energy* **2007**, *32*, 4005.
(21) Wong-Foy, A. G.; Matzger, A. J.; Yaghi, O. M. Exceptional H_2 saturation uptake in microporous metal-organic frameworks. *J. Am. Chem. Soc.* **2006**, *128*, 3494.
(22) Li, Y.; Yang, R. T. Gas adsorption and storage in metal-organic framework MOF-177. *Langmuir* **2007**, *23*, 12937.
(23) Wei, Z.; Hui, W.; Taner, Y. Enhanced H_2 adsorption in isostructural metal-organic frameworks with open metal sites: Strong dependence of the binding strength on metal ions. *J. Am. Chem. Soc.* **2008**, *130*, 15268.
(24) Srinivas, G.; Zhu, Y.; Piner, R.; Skipper, N.; Ellerby, M.; Ruoff, R. Synthesis of graphene-like nanosheets and their hydrogen adsorption capacity. *Carbon* **2010**, *48*, 630.
(25) Takagi, H.; Hatori, H.; Soneda, Y.; Yoshizawa, N.; Yamada, Y. Adsorptive hydrogen storage in carbon and porous materials. *Mater. Sci. Eng., B* **2004**, *108*, 143.
(26) Hirsher, M.; Panella, B.; Schimtz, B. Metal organic frameworks for hydrogen storage. *Microporous Mesoporous Mater.* **2010**, *129*, 335.
(27) Hirsher, M.; Panella, B. Hydrogen physisorption in metal organic porous crystals. *Adv. Mater.* **2005**, *17*, 538.
(28) Luzan, S. M.; Talyzin, A. V. Hydrogen adsorption in Pt catalyst/MOF-5 materials. *Microporous Mesoporous Mater.* **2010**, *135*, 201.
(29) Ping, S.; Yaoqi, L.; Bei, H.; Junzhi, Y.; Jie, Z.; Xingguo, L. Hydrogen storage properties of two pillared-layer Ni(II) metal-organic frameworks. *Microporous Mesoporous Mater.* **2011**, *142*, 208.
(30) Sumida, K.; Brown, C. M.; Herm, Z. R.; Chavan, S.; Bordig, S.; Long, J. R. Hydrogen storage properties and neutron scattering studies of Mg_2(dobdc) a metal–organic framework with open Mg^{2+} adsorption sites. *Chem. Commun.* **2011**, *47*, 1157.
(31) Gumma, S.; Talu, O. Net Adsorption: A thermodynamic framework for supercritical gas adsorption and storage in porous solids. *Langmuir* **2010**, *26* (22), 17013.
(32) Mishra, P.; Edubilli, S.; Mandal, B.; Gumma, S. Adsorption of CO_2 , CO, CH_4 and N_2 on DABCO based metal organic frameworks. *Microporous Mesoporous Mater.* **2013**, *169*, 75.
(33) Fluid properties of Hydrogen, Isothermal Process. http://webbook.nist.gov/chemistry/ (accessed on March 1, 2013).
(34) Rondeau, R. E. Slush baths. *J. Chem. Eng. Data* **1966**, *11*, 124.
(35) Camille, P.; Teresa, J. B. MOF–Graphite Oxide Composites: Combining the Uniqueness of Graphene Layers and Metal–Organic Frameworks. *Adv. Mater.* **2009**, *21*, 4753.
(36) Bimbo, N.; Ting, V. P.; Kolodziejczyk, A. H.; Mays, T. J. Analysis of hydrogen storage in nanoporous materials for low carbon energy applications. *Faraday Discuss.* **2011**, *151*, 59.
(37) Schlapbach, L.; Zuttel, A. Hydrogen-storage materials for mobile applications. *Nature* **2001**, *414*, 353.

Supporting Information

Hydrogen Adsorption on Zn-BDC, Cr-BDC, Ni-DABCO and Mg-DOBDC Metal Organic Frameworks

Debjyoti Sahu, Prashant Mishra, Satyannarayana Edubilli, Anil Verma, Sasidhar Gumma*

Department of Chemical Engineering, Indian Institute of Technology Guwahati, Guwahati - 781039, Assam, India.

Material Synthesis

Zn-BDC also known as IRMOF-1 was synthesized as per procedure suggested in the literature [1]. 2.4 g of zinc nitrate hexahydrate ($Zn(NO_3)_2.6H_2O$, Sigma–Aldrich) and 0.668 g of (H_2BDC, Merck) were dissolved in 80 cm^3 of N,N-dimethyl formamide (DMF, Merck) under mild stirring. After few minutes 4.4 cm^3 of triethyl amine (TEA, Merck) was slowly added to the solution under stirring. After 2 h of stirring the solution was filtered off, washed three times with DMF, and dried in the oven maintained at 378 K for 20 h to obtain IRMOF-1 crystals.

Cr-BDC also known as MIL-101 was synthesized as per reported literature [2]. 4 g of chromium nitrate nonahydrate ($Cr(NO_3)_3{\cdot}9H_2O$, Loba Chemie) was dissolved in 48 cm^3 deionized water followed by addition of 1.64 g H_2BDC. After stirring this solution for some time 0.5 cm^3 hydrofluoric acid was added drop wise while stirring continued for another 15 minutes. The complete solution was then transferred to Teflon-lined stainless steel reactors (autoclave) and sealed. The reactors were placed inside a hot air oven at 493 K and held for 8 h. A fine green colored powder was obtained; excess H_2BDC were still present in the form of needle-shaped crystals. To remove this H_2BDC, DMF was added incrementally with continuous stirring. Filtered product was dried at 423 K overnight. To remove H_2BDC further, an additional ethanol rinse was performed. About 200 mg of the dried product was mixed with 15 cm^3 ethanol in a 60 cm^3 vial and kept at 373 K for 20 h. After cooling, the resulting product was filtered and washed with ethanol. The product was dried finally at 423 K overnight.

Ni-DABCO was synthesized as reported earlier [3]. A mixture of 0.872 g nickel nitrate hexahydrate ($Ni(NO_3)_2{\cdot}6H_2O$, Merck), 0.499 g H_2BDC, (3 mmol, Merck), 0.279 g 1,4-diazabicyclo 2,2,2-octane (DABCO, 2.49 mmol, Alfa Aesar) and 60 cm^3 DMF, was taken in a conical flask at room temperature and stirred for about 10 min. This mixture was then transferred

into an autoclave. The autoclave was placed inside oven at 383 K and held for 24 h. Then it was cooled to room temperature; the green color solid product was filtered and washed thoroughly with DMF followed by drying at ambient temperature (290–303 K) under vacuum.

Mg-DOBDC was synthesized as per procedure suggested in the literature [4,5]. A solid mixture of 0.793g 2,5 dihydroxy benzene dicarboxilic acid (H_4DOBDC, Sigma-Aldrich) and 3.3915 g magnesium nitrate hexahydrate ($Mg(NO_3)_2.6H_2O$, Merck) was added to 357 cm^3 solution of DMF, Ethanol and Water of 15:1:1 volumetric ratio and mixed by sonication for 15 to 20 minutes. This mixture was transferred to twelve 60 cm^3 vials, sealed properly and then kept at 398 K in a hot air oven for 20 h. Obtained yellowish product was decanted slowly and added with 30 cm^3 of methanol in each vial. Entire solution was collected in one reagent bottle and methanol was decanted for four times in next two days. Finally the yellow precipitate is dried in vacuum over hours before it was transferred to inert condition.

TGA analysis

Thermogravimetric analysis (TGA) of synthesized samples (Figure S1) was performed to study the thermal stability of the products. A Mettler TOLEDO analyzer (Model No. TGA/SDTA851^e) was used for analysis of Mg-DOBDC, Ni-DABCO and Cr-BDC whereas Zn-BDC analysis was carried out in a NETZSCH analyzer (Model No. STA449 F3 Jupiter). The initial weight loss (below 373 K) for all of the samples corresponds to the moisture removal. All samples are then stable up to at least 620 K. At higher temperature, sharp decrease in the weight of samples (except Zn-BDC) indicates the decomposition of the materials.

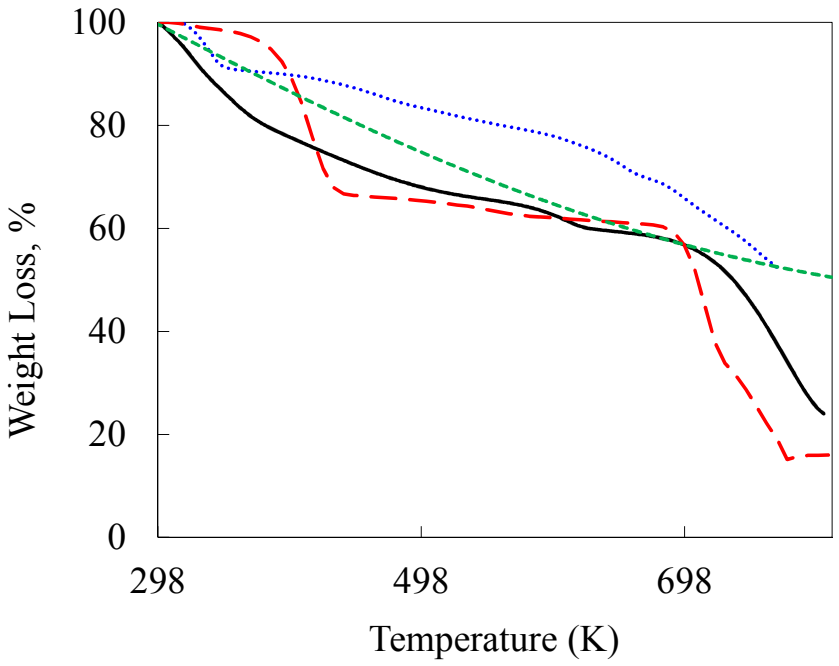

Figure S1. TGA analysis of Zn-BDC (--), Cr-BDC (··), Ni-DABCO from Mishra et.al. [3] (--) and Mg-DOBDC (**--**) under flow of N_2.

XRD Analysis

Powder X-ray diffraction measurements were carried out of synthesized materials using monochromatic Cu-Kα radiation source (λ=1.54178 Å). Dry powder samples were loaded for analysis at atmospheric condition. Specimens were scanned between 1^{o} to 45^{o}. XRD patterns obtained in this work are compared with that available in the literature to confirm the synthesis of the samples. It was observed that XRD patterns obtained in this work (Figure S2) match well with those reported in literature for Zn-BDC [6], Cr-BDC [7], Ni-DABCO [8], Mg-DOBDC [4].

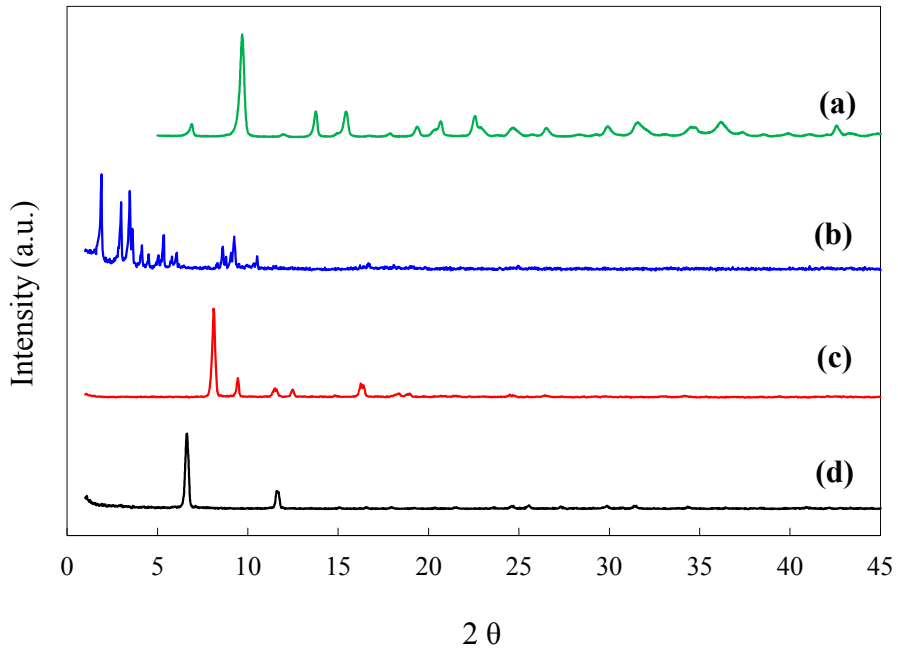

Figure S2. Powder XRD pattern for (a) Zn-BDC, (b) Cr-BDC, (c) Ni-DABCO and (d) Mg-DOBDC MOFs.

BET analysis

The BET surface area and pore volume measurements of Zn-BDC, Ni-DABCO and Cr-BDC were done using a surface area analyzer (Beckman–Coulter SA3100). For Mg-DOBDC, Quantachrome autosorb-iq was used. Prior to measurement of N_2 isotherms at 77 K (Figure S3) in surface area analysis, all samples were out-gassed under vacuum at higher temperatures for sufficient time (please see table S2 for more details). The relative pressure (Ps/P_0) range between 0.05 and 0.2 was used in the BET surface area calculation. The pore volume calculation was performed at a pre-determined relative pressure (P/P_s) of 0.98.

Table S1. BET surface area and pore volume.

Compound	Open metal site	Activation temperature, K	Activation time, h	surface area, $m^2\ g^{-1}$	pore volume, cc g^{-1}	Ref.
Zn-BDC	No	393	-	832	0.3	[1]
		-	-	500.8	0.19	[6]
		398	6	2833	1.13	[9]
		393	6	623	0.38	present study
Cr-BDC	Yes	403	3	2674	1.38	[2]
		-	-	2931	1.45	[10]
		473	1.5	2930	1.52	present study
Ni-DABCO	No	453	3	1904	0.98	[3]
Mg-DOBDC	Yes	-	-	1800	0.57	[11]
		-	-	1332	0.61	[5]
		473	3	1085	0.66	present study

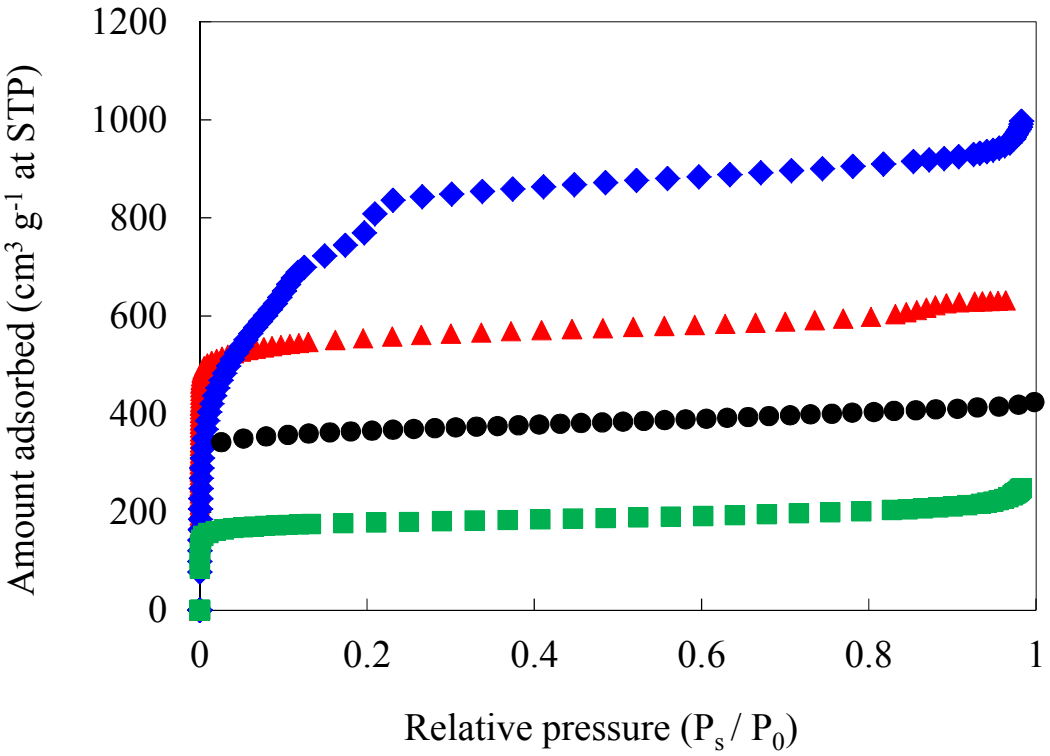

Figure S3. N_2 physisorption study at77 K for Zn-BDC (■), Cr-BDC (♦), Ni-DABCO from Mishra et al. [3] (▲) and Mg-DOBDC (●).

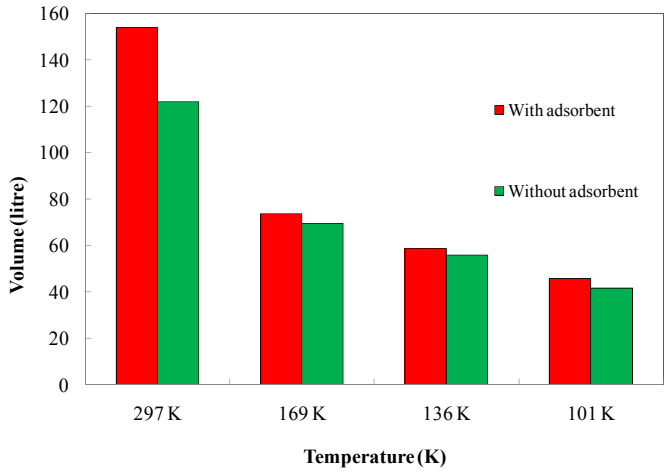

Fig S4: Tank volume required to store 1 kg of hydrogen with Zn-BDC as adsorbent

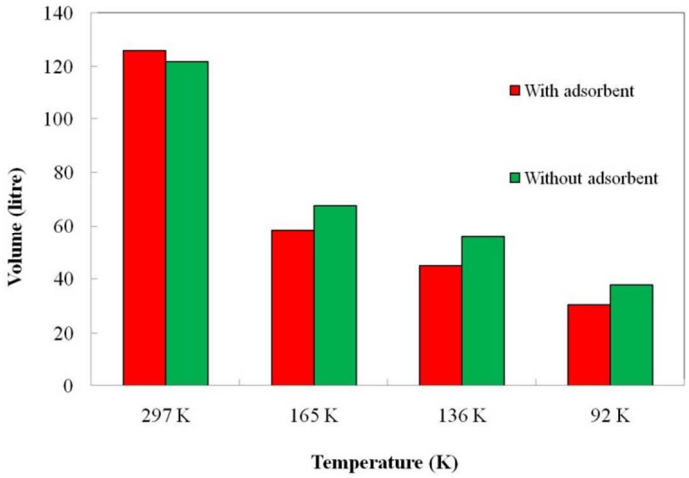

Fig S5: Tank volume required to store 1 kg of hydrogen with Cr-BDC as adsorbent

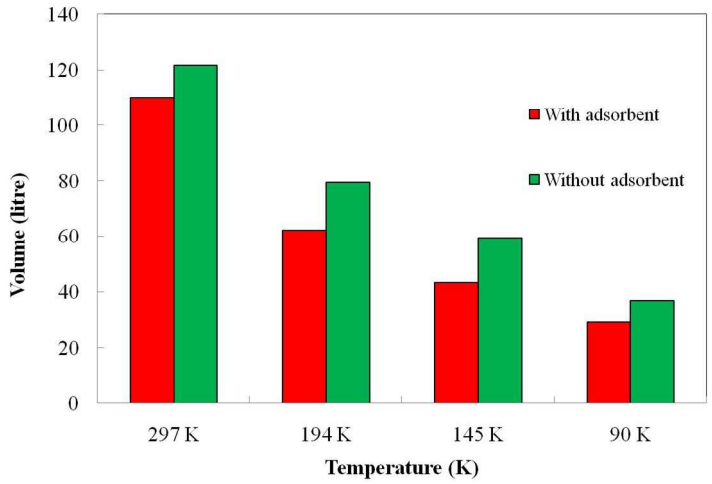

Fig S6: Tank volume required to store 1 kg of hydrogen with Ni-DABCO as adsorbent

References

[1] Luzan, S. M.; Talyzin, A. V.; Microporous Mesoporous Mater., 2010, 135, 201.

[2] Chowdhury, P.; Bikkina, C.; Gumma, S.; J. Phys. Chem. C, 2009, 113, 6616.

[3] Mishra, P.; Edubilli, S.; Mandal, B.; Gumma S.; Microporous Mesoporous Mater., 2013, 169, 75.

[4] Wei, Z.; Hui, W.; Taner, Y.; J. Am. Chem. Soc.; 2008, 130, 15268.

[5] Hui, W.; Wei, Z.; Taner, Y.; J. Am. Chem. Soc.; 2009, 131, 495.

[6] Jinping, L.; Shaojuan, C.; Qiang, Z.;Peipei, L.; Jinxiang, D.; Int. J. Hydrogen Energy, 2009, 34, 1377.

[7] Liu, Y. Y.; Zeng, J. L.; Zhang, J.; Xu, F.; Sun, L. X.; Int. J. Hydrogen Energy, 2007, 32, 4005.

[8] Ping, S.; Yaoqi, L.; Bei, H.; Junzhi, Y.; Jie, Z.; Xingguo, L.; Microporous Mesoporous Mater., 2011, 142, 208.

[9] Andrew, R. M.; Yaghi, O. M.; J. Am. Chem. Soc. 2005,127, 17998.

[10] Li, Y.; Yang, R. T.; AIChE Journal 2008, 54, 269.

[11] Jarad, A. M.; Kenji, S.; Zoey, R. H.; Rajamani, K.; Jeffrey. R. L.; Energy Environ. Sci., 2011, 4, 3030.